

APOLLO 17 DEEP DRILL CORE 70001/9: LARGE IMPACT AGES AT TAURUS-LITTROW, RECORDED INCREASE IN SOLAR LUMINANCE, AND IMPLICATIONS FOR ANGSA STUDIES.

Schmitt, H. H., University of Wisconsin-Madison, P. O. Box 90730, Albuquerque NM 87199

hhschmitt@earthlink.net

Introduction: Synthesis of published data on maturity indices [1] with petrographic characteristics [2,3,4,5,6], volatile element concentrations [7,8], and nitrogen isotopic measurements [9] provides new insights into the depositional and exposure history of regolith sampled by the Apollo 17 deep drill core (70001/9) [10]. The 285 cm deep core records the impact and maturation history of Taurus-Littrow regolith. The core also records a major increase in solar wind spallation at about 0.5 Ga [11].

Maturity Indices (MI): The MI (Is/FeO) given by Morris [1], down the Apollo 17 deep drill core, indicate regolith zones of significantly different degrees of exposure to solar wind spallation and micro-meteor impact [12]. This current study uses the MI variations to delineate 8 specific regolith zones in the core (Table 1). A major increase or decrease in average MI defines the top of each zone. Small spikes showing an increase over a zone's average MI indicate continuing, post-deposition maturation preceded by redistribution of relatively small amounts of ejecta having the average MI of the zone.

Petrography: Detailed petrography of each of the MI defined zones (Table 1) corresponds with the definition of zones based on MI data. Note (1) the concentration of coarse rock fragments [2] and high Zn [7] reported in Zone T that indicates derivation from a relatively immature regolith source, such as the Crater Cluster area to the south and east of the drill site, (2) marked variations in ash content between various zones, and (3) the presence of material of KREEP and VLT affinities, largely in Zones X, Y and Z [3,6]. The VLT glasses also are present in surface regolith samples from near the Sculptured Hills where pyroclastic fissures have been identified [13].

Nitrogen Isotopes: Plotting measured $\delta^{15}\text{N}\%$ [9] for the 8 defined zones against MI (Table 2, Fig. 1) shows a direct correlation in the lower 5 zones, with $\delta^{15}\text{N}\%$ increasing with increasing MI along a slope of +1.23‰/MI. Using this rate of change of +1.23‰ per MI increase to correct $\delta^{15}\text{N}\%$ values for preferential loss of ^{14}N during maturation gives original values of -107 ± 7 for $\delta^{15}\text{N}\%$ in Zones V-Z (Column 6 in Table 2).

Conversely, the younger three zones, S-U, require a correction related to a $\delta^{15}\text{N}\%$ /MI ratio of $\sim +2.67$ to match the -107 ± 7 values for solar $\delta^{15}\text{N}\%$ indicated by older zones (Fig. 1). Using this higher ratio to control the slope of a line through points for S-U in Fig. 1, gives an intercept of $\sim \delta^{15}\text{N}\% = \sim -107$ at zero MI.

Extrapolated Ages of Impact Events: The change in MI (ΔMI) after deposition of each zone can be

estimated from totaling the MI spikes above average MI for each zone (Column 3, Table 3).

Table 1. Stratigraphic zones and related samples in the deep drill core as indicated by variations in maturity index (MI), ash content, and selected petrographic characteristics.

Z o n e	Location (cm) (Sample)	MI (Is/ FeO)	Ash %	Other Petrographic Characteristics (Apparent Source Crater)
S	0-18 (70009)	47	8	(Local Small Craters)
T	22-55 (70008)	12	20	Course rock fragments, high orange+black ash, low Al_2O_3 and high Zn. (Crater Cluster)
U	55-85 (70007)	38	24	High orange+black ash and high Al_2O_3 and high Zn. (Camelot)
V	85-115 (70007/6)	53	15	Variable orange+black ash (Lara or Pre-Cluster)
W	115-173 (70006/5):	83 75	13 16	Variable orange+black ash, high agglutinates, and very low Zn. (Horatio)
X	173-220 (70005/4)	65	20	Enhanced KREEP and both orange+black ash and green VLT ash. (Henry)
Y	220-255 (70003)	45	13	Enhanced KREEP and both orange+black and green VLT ash. (Cochise)
Z	255-285 (70003/2/1)	53	13	Enhanced KREEP and both orange+black ash and green VLT ash. (Shakespeare)

Table 2. Stratigraphic zones and related samples in the deep drill core showing the relations of reported $\delta^{15}\text{N}\%$ and maturity indices. $\delta^{15}\text{N}\%$ values corrected for ^{14}N loss (see Fig. 1) are given in the last column.

Z o n e	Location (cm) (Sample)	MI	N Analysis Depth (cm)	Implanted $\delta^{15}\text{N}\%$	$\delta^{15}\text{N}\%$ [9] Corrected for old MI Loss Rate [New Loss Rate]
S	0-18 (70009)	47	13.6-15.1	+19	-39 [-106]
T	22-55 cm (70008)	12	41.4-44.3	-73.6	-89 [-106]
U	55-85 (70007)	27	60.3-62.5	-56.0	-89 [115] Camelot (0.5±0.2 Ga)
V	85-115 (70007/6)	53	86.4-87.9	-45.1	-110
W	115-173 (70006/5)	83 75	119.2-120.9 137.8-139.3	-11.8 -8.0	-114 -100
X	173-220 (70005/4)	65	176.2-177.7	-21.1	-101
Y	220-255 (70003)	45	231.7-233.3	-53.8	-109
Z	255-285 (70003-1)	53	269.7-271.2	-40.9	-106

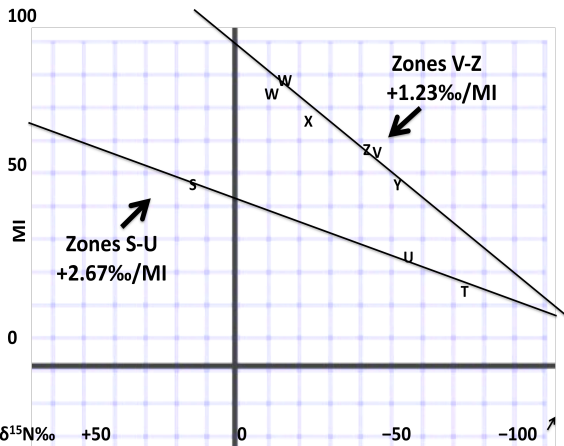


Fig. 1. Plot of $\delta^{15}\text{N}\text{‰}$ vs. Maturity Index (MI) shows a $\sim +1.22\text{‰/MI}$ correlation for deep drill core zones except S-U for which a $\sim +2.67\text{‰/MI}$ correlation is indicated [after 11].

An estimated change in maturity index per million years (Column 4, Table 3) then can be calculated using an topographic diffusion age of Camelot Crater of 0.5 ± 0.2 Ga [13] (Zone U). Dividing 500 Myr by 89, the total of ΔMI for Zones S-U, give an estimated $\Delta\text{MI/Myr}$ of 0.178 for those 3 zones. The change between zones U and V from the old $+1.23 \delta^{15}\text{N}\text{‰/MI}$ ratio to the current faster rate of $+2.67\text{‰/MI}$ (Fig. 1), a factor of 2.17, gives the slower rate of $\Delta\text{MI/Myr}$ of 0.082 for lower Zones V-Z. Based on these rates, the estimated post-deposition exposure ages of each zone can be calculated (Column 5, Table 3).

The relative ages of major potential source craters can be determined from differences in topography and boulder distributions and size-frequencies on crater rims and interior walls. The author's review of LROC Narrow Angle Camera images and his direct observations and photography during Apollo 17 EVAs indicate that the relative crater age sequence from older to younger is: Shakespeare, Cochise, Henry-Horatio, Camelot, Crater Cluster, and local small craters. The approximate age of each zone's probable source crater thus can be determined by summing the exposure ages in sequence (Column 6, Table 3). The estimated ~ 3.266 Ga age of the oldest zone, Zone Z, is less than that estimated for the demise of the Moon's strong, protective magnetic field at 3.56 Ga [14], allowing for a significant level of regolith maturation at the apparent source crater site (Shakespeare).

Solar Luminance Increase: The increased rate of maturation shown by the 3 upper regolith zones in the deep drill core indicates that the rate of solar wind spallation of lunar surface materials increased by a factor of ~ 2.17 about 0.5 Ga and appears to have remained constant since. This apparent increase in solar luminance or the frequency of energetic solar flares and/or coronal mass ejections occurred about the

same time as the Cambrian Explosion on Earth [15], when there was a sharp increase in the quantity and diversity of life in the oceans. The question remains as to whether these two phenomena could be related.

Table 3. Stratigraphic zones and related samples in the deep drill core showing an estimated sum of changes in maturity index (ΔMI) per million years (see text). (Location of zones in core and related samples given in Table 1.)

Z o n e	MI Pre- -	ΔMI Post- (Est.)	$\Delta\text{MI/}$ Myr, (Est.)	Exposure Age (Myr) (Est.)	Source Crater Age (Ga) (Est.)
S	~ 44	70	0.178	393	0.393
T	~ 8	7	0.178	39	0.432 Cluster
U	~ 33	12	0.178	67	0.5 ± 0.2 Camelot
V	~ 65	27	0.082	329	0.829 Lara (?)
W	~ 63	31	0.082	378	1.207 Horatio
X	~ 51	73	0.082	890	2.097 Henry
Y	~ 54	39	0.082	476	2.573 Cochise
Z	~ 54	56	0.082	693	3.266 Shakespeare

Conclusions:

- Stratigraphy of introduced regolith in the deep drill core can be documented through detailed synthesis of maturity indices with other data.
- Core $\delta^{15}\text{N}\text{‰}$ values increase linearly with MI indicating a loss of 14N with increases in maturation.
- Correlation of a regolith zone with the dated Camelot Crater (0.5 ± 0.2 Ga) provides the approximate exposure ages of other zones in the core and absolute ages of source craters.
- Solar history recorded in cores will benefit from precise as possible topographic diffusion ages [16] of impact craters < 1 km in diameter.
- A factor of ~ 2.17 increase in solar wind energy by occurred at about 0.5 ± 0.2 Ga.

References: [1] Morris, R. V., et al., (1979) *PLPSC 10*, 1141-1157. [2] Laul, et al., (1978) *PLPSC 9*, 2065-2097. [3] Vaniman, D. T., et al., (1979) *PLPSC 10*, 1185-1227. [4] Taylor, G. J., et al., (1979) *PLPSC 10*, 1159-1184. [5] Heiken, G. H., et al., (1992) *Lunar Source Book*, 335-392. [6] Vaniman, D. T., and Papike, J. J., (1977) *PLSC 8*, 1443-1471. [7] Laul, J. C., and Papike, J. J. (1980) *PLPSC 11*, 1269-1298. [8] Krähenbühl (1980) *PLPSC 11*, 1551-1564. [9] Thieme, M. H., and Clayton, R. N. (1980) *PLPSC XI*, 1438-1439, Table 1. [10] Baldwin, R. R., (1973) *Apollo 17 Prelim. Sci. Rept.*, 2.4. [11] Schmitt, H. H. (2019) Masursky Lecture, *PLPSC LI*. [12] Pieters, C. M., et al. (2000), *Met. & Planet. Sci.* 35, 1101-1107. [13] Schmitt, H. H., (2017) *Icarus*, 298, 1-19. [14] Tikoo S. M., et al. (2017) *Sci. Adv.*, 3, 1-9 [15] Maloof, A. C., et al. (2010) *GSA Bull.* 122, 1731-1774. [16] Fassett, C. I., & Thompson, B. J. (2014), *Jour. Geophys. Res.* 119, 2255-2271.